

# 1 The Observed Evolution of Arctic Amplification over the Past 45 2 Years

3 Mark C. Serreze<sup>1</sup>, Elizabeth Cassano<sup>1,2</sup>, Alex Crawford<sup>3</sup>, John J. Cassano<sup>1,2</sup>, and Chen Zhang<sup>1,2</sup>

4 <sup>1</sup>Cooperative Institute for Research in Environmental Sciences, National Snow and Ice Data Center, University of Colorado  
5 Boulder, CO, USA

6 <sup>2</sup>Department of Atmospheric and Oceanic Sciences, University of Colorado Boulder, Boulder, CO, USA

7 <sup>3</sup>Centre for Earth Observation Science, Department of Environment and Geography, University of Manitoba, Winnipeg, MB,  
8 Canada

9  
10 *Correspondence to:* Mark Serreze (mark.serreze@colorado.edu)

11 **Abstract.** To address research gaps in understanding Arctic Amplification, we use data from ERA5, an observational surface  
12 temperature dataset, and sea ice concentration to examine the seasonal, spatial and decadal evolution of Arctic 2-meter and  
13 lower tropospheric temperatures and lower tropospheric (surface to 850 hPa) static stability over the past 45 years. A Local  
14 Amplification Anomaly (LAA) metric is used to examine how spatial patterns of Arctic 2-meter temperature anomalies  
15 compare to anomalies for the globe as a whole. Pointing to impacts of seasonally-delayed albedo feedback, growing areas of  
16 end-of-summer (September) open water largely co-locate with the strongest positive anomalies of 2-meter temperatures  
17 through autumn and winter and their growth through time; small summer trends reflect the effects of a melting sea ice cover.  
18 Because of seasonal ice growth, the association between rising 2-meter temperatures and sea ice weakens from autumn into  
19 winter, except in the Barents Sea where there have been prominent downward trends in winter ice extent. Imprints of variable  
20 atmospheric circulation are prominent in the Arctic temperature evolution. Low-level (surface to 850 hPa) stability over the  
21 Arctic increases from autumn through winter, consistent with the greater depth of surface-based atmospheric heating seen in  
22 autumn. However, trends towards weaker static stability dominate the Arctic Ocean in autumn and winter, especially over  
23 areas of September and wintertime ice loss. Sea ice thinning, leading to increased conductive heat fluxes through the ice, likely  
24 also contributes to reduced stability.

## 25 26 27 **Non-technical Summary**

28 The outsized warming of the Arctic relative to the globe as a whole (Arctic Amplification) is largest in autumn and winter,  
29 consistent with large transfers of energy from growing areas of open water. Impacts of variable atmospheric circulation are  
30 also prominent. AA is small in summer due to the melting sea ice cover. Warming penetrates higher into the atmosphere in  
31 autumn compared to winter, but trends towards weaker stability could enable deeper heating as AA further evolves.

32

33

## 34 **1 Introduction**

35 Arctic amplification (AA) refers to the observation that, over the last several decades, the rate of increase in surface air  
36 temperature over the Arctic region has been larger than for the globe as a whole. As reviewed by Esau et al. (2023), AA is  
37 having impacts on Arctic terrestrial and marine ecosystems, permafrost conditions, ice sheets and glaciers as well as human  
38 systems. AA was predicted as a consequence of global warming even in the earliest generation of climate models, and was  
39 envisioned as far back as the 19<sup>th</sup> century (Arrhenius, 1896). Various studies have placed the ratio of Arctic to global warming  
40 from two to four, with differences relating to the definition of the Arctic region, data used, the time period examined and the  
41 season examined (Yu et al., 2021a; Walsh, 2014; Richter Menge and Druckenmiller, 2020; Jansen et al., 2020; AMAP, 2021;  
42 Rantanen et al., 2022). Using several observational data sets and defining the Arctic as the region poleward of the Arctic Circle,  
43 Rantanen et al. (2022) find a factor of four warming relative to the globe over the period 1979-2021 based on annual mean  
44 temperatures. From comparisons with climate models, they conclude that this large ratio is either an extremely unlikely event,  
45 or that the models systematically underestimate AA. Zhou et al. (2024) conclude that the externally forced amplification is  
46 three-fold, with natural variability explaining the remainder. The Polar Amplification Model Intercomparison Project (PAMIP;  
47 Smith et al., 2019) further investigates the causes and consequences of polar amplification using a coordinated set of numerical  
48 model experiments, providing valuable insights into the mechanisms driving AA.

49 Growing spring and summer sea ice loss, leading to more seasonal heat gain in the ocean mixed layer and subsequent upward  
50 heat release in autumn and winter - a seasonally-delayed expression of albedo feedback - is widely accepted as a key driver of  
51 AA (Perovich et al., 2007; Steele et al., 2008; Serreze et al., 2009; Screen and Simmonds, 2010a,b; Stammerjohn et al., 2012;  
52 Stroeve et al., 2014, Dai et al., 2019). However, based on observations and modeling studies, AA is also recognized as  
53 involving a suite of connected contributions including changes in atmospheric circulation and poleward energy transport  
54 (Graversen and Burtu, 2016; Woods and Caballero, 2016; Henderson et al., 2021; Previdi et al., 2021, Zhang et al., 2025),  
55 Planck feedback (Pithan and Mauritsen, 2014), positive lapse rate feedback (Pithan and Mauritsen, 2014; Stuecker et al., 2018;  
56 Previdi et al., 2021), changes in ocean heat transport (Beer et al., 2020), changes in autumn cloud cover (Kay and Gettelman,  
57 2009; Wu and Lee, 2012) and even reduced air pollution in Europe (Navarro et al., 2016; Krishnan et al., 2020). Taylor et al.  
58 (2022) provide an insightful history of AA science.

59 However, much remains to be understood about AA, notably the spatial aspects of its observed evolution, seasonal shifts in its  
60 expression and evolution, and the vertical structure of AA in the context of changing static stability. Here, using data from the  
61 ERA5 reanalysis, surface temperature observations, and satellite-derived sea ice concentration, we focus on understanding the  
62 decadal evolution and seasonal/spatial expressions of Arctic temperature anomalies. The local characteristics of AA are

63 important, as regional variations can produce different remote influences, including midlatitude climate extremes (Zhou et al.,  
64 2023). We show how: 1) the pronounced autumn contribution to AA, through which internal energy gained by the upper ocean  
65 in spring and summer in growing open water areas is subsequently released back to the atmosphere, decays into winter as sea  
66 ice forms (the exception being in the Barents Sea sector, which has seen pronounced winter ice losses; 2) The decadal evolution  
67 of AA is modulated by variable spatial expressions of atmospheric circulation; 3) the deeper vertical extent of pronounced  
68 temperature anomalies in autumn than winter is consistent with the seasonal increase in static stability from autumn to winter;  
69 and 4) reductions in static stability in autumn point toward increasingly deep penetration of surface warming into the  
70 troposphere with continued sea ice loss, and potentially greater impacts of AA on altering weather patterns in lower latitudes  
71 (Ding et al., 2024).

## 72 **2 Data Sources**

73 Data from the European Centre for Medium-range Weather Forecasts (ECMWF) reanalysis (ERA5; Hersbach et al., 2020) are  
74 used for analysis. Monthly temperature (2 m and the significant levels from 1000 to 500 hPa) and surface and latent heat fluxes  
75 were used on the 0.25° x 0.25° horizontal grid from 1979-2024. While ERA5 data are available since 1950, fields since 1979,  
76 the advent of the modern satellite database for assimilation, are more reliable. ERA5 is chosen because, in various comparisons  
77 of (near-) surface parameters throughout the Arctic, ERA5 performs similarly to or better than other global and regional  
78 reanalysis products (Graham et al., 2019; Barrett et al., 2020; Renfrew et al., 2021; Crawford et al., 2022). Reliance is placed  
79 on trends and anomalies. Anomalies are referenced to the 30-year period 1981-2010, but comparisons are made with different  
80 averaging periods. To assess relationships with sea ice conditions, we use the satellite passive microwave records from the  
81 National Snow and Ice Data Center. The satellite passive microwave record provides estimates of concentration and extent  
82 from October 1978 through the present at 25-km resolution on a polar stereographic grid by combining data from the Nimbus-  
83 7 Scanning Multichannel Microwave Radiometer (SMMR, 1979–1987), the Defense Meteorological Satellite Program  
84 (DMSP) Special Sensor Microwave/Imager (SSM/I, 1987–2007) and the Special Sensor Microwave Imager/Sounder (SSMIS,  
85 2007-onwards) (Fetterer et al., 2002).

86  
87 Our results must be viewed within the context of known problems in ERA5, one being a warm bias in 2-meter air temperature  
88 over the Arctic (Yu et al., 2021b; Tian et al., 2024). Compared to an extensive set of matching drifting observations, Yu et al.  
89 (2021b) found ERA5 to have a mean bias of  $2.34 \pm 3.22$  °C in 2-meter air temperature, largest in April and smallest in  
90 September. Interestingly, surface (skin) temperature biases were found to be negative ( $-4.11 \pm 3.92$  °C overall, largest in  
91 December and smaller in the warmer months), although the magnitudes might be overestimated by the location of the surface  
92 temperature sensors on the buoys, which may have been affected by snow cover. While we are largely dealing in this paper  
93 with anomalies, rather than absolute values, our comparisons between Arctic and global anomalies may be influenced by the  
94 fact that biases at the global scale are different. Wang et al. (2019) found that compared to the earlier ERA-I effort, ERA5 has

95 a larger warm bias at very low temperatures ( $< -25^{\circ}\text{C}$ ) but a smaller bias at higher temperatures. ERA5 has higher total  
96 precipitation and snowfall over Arctic sea ice. The snowpack in ERA5 results in less heat loss to the atmosphere and hence  
97 thinner ice at the end of the growth season, despite the warm bias.

98

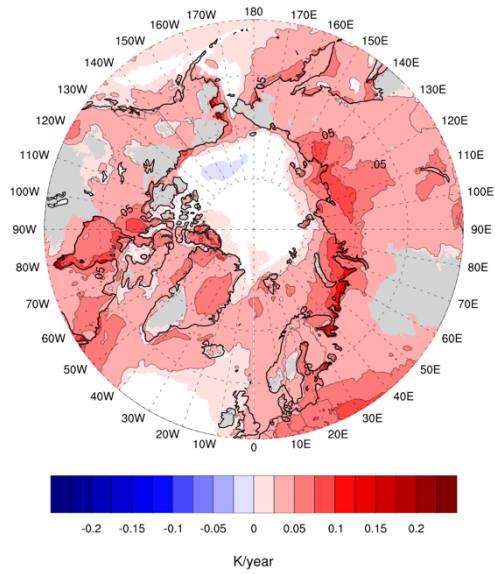
99 To further address biases in ERA5, analysis was also performed using the Berkeley Earth Surface Temperatures (BEST)  
100 gridded surface temperature data (Rohde and Hausfather, 2020; Available for download from: <https://berkeleyearth.org/data/>).  
101 This dataset extends back to 1850, combining both 2m temperatures over land as well as sea surface temperatures to create a  
102 global, gridded observational dataset to which reanalysis data can be compared.

### 103 **3 Results**

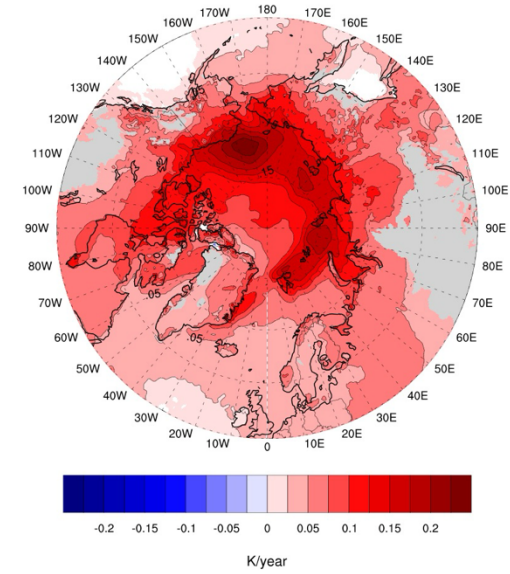
#### 104 **3.1 Seasonality of 2-Meter Temperature Trends**

105 A key, but in our view, under-appreciated aspect of AA is its strong seasonality - under-appreciated not that it exists but in the  
106 sense that processes at work during summer over the Arctic Ocean, when AA is small, set the stage for understanding the  
107 strong imprints of AA during autumn and winter. Rantanen et al. (2022) found that the AA factor as assessed for the region  
108 poleward of the Arctic circle ranges from less than 2 in July to over 5 in November. Climate models examined in that study  
109 largely capture this seasonality but with smaller amplification factors. Figure 1 shows spatial patterns of surface air temperature  
110 trends by season based on ERA5. In this study, the Arctic is defined as areas poleward of  $60^{\circ}\text{N}$ , but maps extend down to  $50^{\circ}\text{N}$   
111 to enable comparisons between changes in the Arctic and the higher middle latitudes. The same analysis but performed with  
112 the BEST data are shown in Supplemental Figure 1. The description of the results from these figures apply to both datasets  
113 except where explicitly stated.

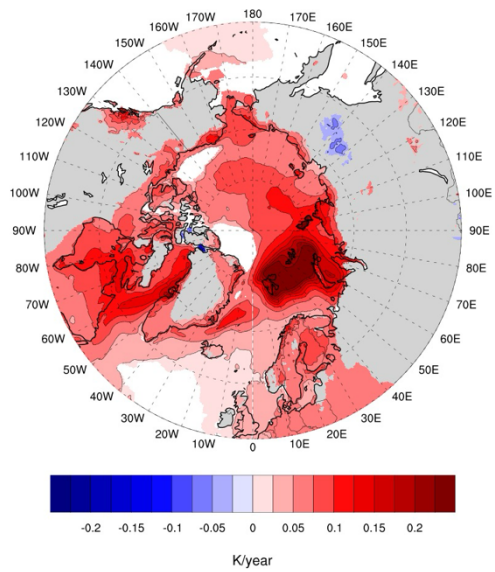
**(a) JJA change in T2M /year 1980-2024**



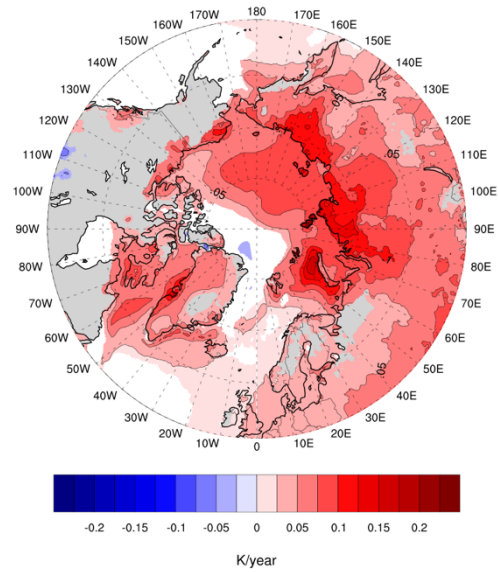
**(b) SON change in T2M /year 1980-2024**



**(c) DJF change in T2M /year 1980-2024**



**(d) MAM change in T2M /year 1980-2024**



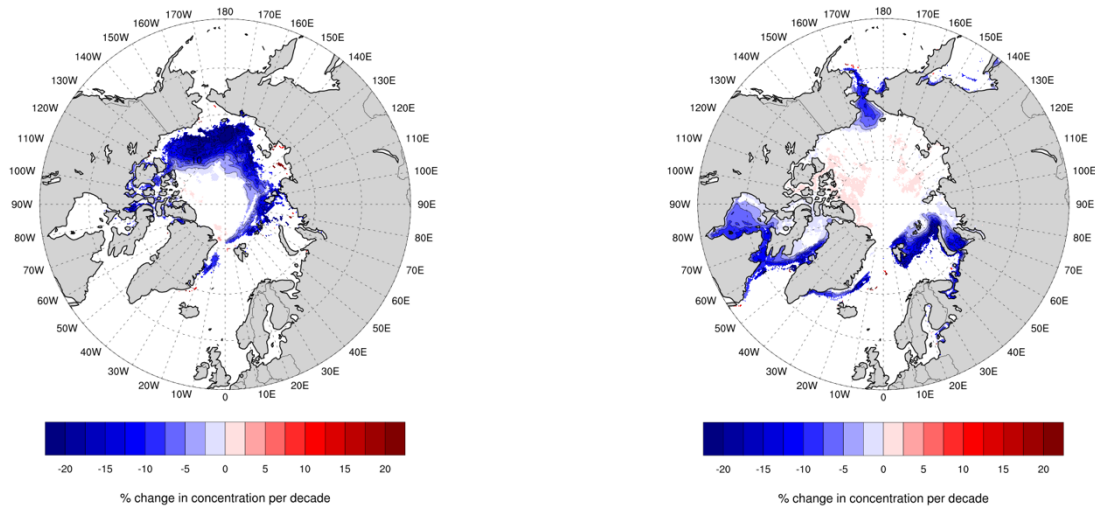
114

115

116

117 **Figure 1: Linear trends in ERA5 2-meter temperatures (T2M) by season from 1980 to 2024, in degrees per year for (a) June, July,**  
118 **August (JJA), (b) September, October, November (SON), (c) December, January, February (DJF) and (d) March, April, May**  
119 **(MAM). Only trends significant at  $p < 0.05$  are shaded based on an ordinary least squares regression test.**

(a) Sep percent change in sea ice concentration/decade 1980-2024 (b) Dec percent change in sea ice concentration/decade 1980-2024



121

122 **Figure 2: Linear trends in sea ice concentration %/per decade 1980 through 2024 for September (a) and December (b). Only**  
 123 **trends significant at  $p < 0.05$  are shaded based on an ordinary least squares regression test.**  
 124

125 The sharply smaller trends in summer compared to autumn and winter across Arctic latitudes clearly stands out. In interpreting  
 126 these patterns, we focus on broad, contiguous regions rather than isolated grid points that may be affected by spatial  
 127 autocorrelation. Summer trends are nevertheless largely positive and statistically significant across most of the Arctic and  
 128 subarctic lands. Trends in ERA5 are very small and not statistically significant across the central Arctic Ocean, while in the  
 129 BEST data, the trends over the Arctic Ocean are significant, albeit still small (Figure S1a). Since the skin temperature of a  
 130 melting sea ice cover is pegged to the melting point, it follows that surface air temperature trends must be small in this area.  
 131 Over land, earlier loss of the snow cover (Mudryk et al., 2023) likely contributes to the rise in surface air temperatures seen  
 132 there. Trends along the Russian and Alaska coastline are also positive. Melt onset typically starts in June in the southern  
 133 margins of the ice cover and progresses poleward (Markus et al., 2009). Positive trends along the coastal seas are consistent  
 134 with satellite observations of a progressively earlier onset of melt (Stroeve et al., 2014; Stroeve and Notz, 2018). They are also  
 135 consistent with progressively earlier exposure of dark open water areas, their expanding coverage through time, and associated  
 136 increased internal energy in the ocean mixed layer (Perovich et al., 2007; Serreze et al., 2009; Perovich and Polashenski, 2012;  
 137 Stammerjohn et al., 2012; Dai et al., 2019; Li et al., 2021; Bianco et al., 2024). However, the large specific heat of water and  
 138 the depth of heating (10-30 m) will limit the rise in surface air temperature. Note also the positive trends over the northern  
 139 North Atlantic, which is ice-free over the entire year. Somewhat larger trends are found over part of the Kara and Barents Seas.

140 The largest temperature trends for autumn, locally exceeding  $0.2^{\circ}\text{C}$  per year, lie primarily on the Eurasian side of the Arctic  
141 Ocean and north of Alaska. A comparison to the spatial pattern of September (end of summer) sea ice concentration (Figure  
142 2), provides an understanding: the trends are largest in those areas with the sharpest downward trends in ice concentration,  
143 most notably in the Chukchi and East Siberian Seas and hence where there will be strong upward surface heat fluxes as the  
144 ocean loses the internal energy it gained in summer. Our interpretation, building from the above discussion and from earlier  
145 studies (e.g., Stammerjohn et al., 2012; Stroeve et al., 2016; Lebrun et al., 2019), is that through the years, ice begins to retreat  
146 earlier and earlier in spring and summer, largely from the shores of Alaska and the Russian coast, exposing areas of dark open  
147 water, which absorbs solar energy. This means more energy gain in the ocean mixed layer, and over an increasingly large area,  
148 with time. As solar radiation declines in autumn, this energy is released upwards to the atmosphere, seen as positive  
149 temperature anomalies that grow in magnitude and spatial coverage with time. Before sea ice forms, all of the internal energy  
150 gained in summer must be depleted.

151 The pattern of winter temperature trends is quite different. The positive trends along the Eurasian coastline and in the Chukchi  
152 and Barents Seas are greatly reduced, and the largest trends, exceeding  $0.2^{\circ}\text{C}$  per year, are now located in the Barents Sea. The  
153 reason for this is clear: by December, the areas of open water along the coast have re-frozen, reducing energy transfer between  
154 the ocean and atmosphere. The Barents Sea is, in turn, one of the few areas with a substantial downward trend in winter sea  
155 ice extent (Figure 2b). Still, positive 2-meter temperature trends in both autumn and winter encompass much of the Arctic  
156 Ocean away from areas of ice loss. One likely driver of this is progressive thinning of the ice cover (Landy et al., 2022; Sumata  
157 et al., 2023), allowing for an increase in conductive fluxes through the ice (Liu and Zhang, 2025). Autumn and winter trends  
158 in sensible and latent heat fluxes from ERA5 show an increase over the time period of study of these fluxes from the surface  
159 to the atmosphere (Supplemental Figure S2). Another driver is likely polar temperature advection from the areas of sea ice  
160 loss (Timmermans et al., 2018), as evidenced by the tongue of fairly large positive trends extending from the Barents Sea into  
161 the Arctic Ocean. Also of interest is that trends over much of the land area are very small, even negative, especially over  
162 Eurasia.

163 By spring, the magnitude of temperature trends in both the ERA5 and BEST data over the Barents Sea has dropped relative to  
164 winter, but is still prominent. Through spring, downward trends in sea ice concentration (not shown) persist, but, compared to  
165 winter, air-sea temperature differences are smaller, hence ocean to atmosphere surface heat fluxes are smaller. Substantial  
166 positive trends are found along the Eurasian coast, again suggestive of the role of atmospheric heat advection. Trends over  
167 much of high-latitude North America are small.

168 To summarize, it is apparent that an assessment of Arctic Amplification based on comparing the Arctic trend with the trend  
169 for the globe as a whole must recognize the highly pronounced seasonal and spatial heterogeneity of Arctic trends. Summer 2-  
170 m temperature trends are mostly small, but the smallness over the Arctic Ocean is due to the melting of ice. The much larger

171 autumn trends reflect energy transfer from the ocean to the atmosphere via upward surface heat fluxes from increasing  
 172 extensive areas of open water. By winter, open water areas along the Eurasian coast and the Chukchi Sea have re-frozen and  
 173 the locus of maximum temperature trends is shifted to the Barents Seas, consistent with the downward trends in sea ice  
 174 concentration there. Spring trends are weaker than winter trends, but are still large in the Barents Sea sector. However, for  
 175 autumn, winter and spring, there are also features in the spatial patterns of trends that point to advection and other processes,  
 176 and winter trends in particular are small over much of the land area.

### 177 3.2 Local Amplification Anomaly Approach

178 To gain further insight into trends, we now look at the evolution of AA by decade, 1980-1989, 1990-1999, 2000-2009, and  
 179 2010-2019, as well as the last five years of the record, 2020-2024, making use of what we term a Local Amplification Anomaly  
 180 (LAA) approach.

181 For each of these periods, we calculated the average 2-meter temperature at each ERA5 and BEST grid point across the globe,  
 182 then calculated the anomalies at each grid point relative to the 1981-2010 climatology. Taking the (spatially weighted) average  
 183 of all grid point anomalies yields the global temperature anomaly for each period. Then, at each grid point we subtracted this  
 184 global temperature anomaly from the anomaly at that point. We then compiled maps of the anomalies for the region poleward  
 185 of 50°N (including the Arctic (north of 60°N) and the sub-Arctic (50-60°N)). Examining these LAAs gives us a sense of the  
 186 spatial structure of Arctic temperature anomalies in terms of how they contribute to the overall AA evolution. In Table 1 we  
 187 also provide, for each decade and season, the average of the anomalies relative to the global average poleward of 60°N and  
 188 the average global anomaly. Results that follow will of course reflect the chosen 1981-2010 referencing period.

	Global Anomaly (K)		Arctic Anomaly (K)		Difference (Arctic – Global; K)	
	BEST	ERA5	BEST	ERA5	BEST	ERA5
Autumn						
1980-1989	-0.22	-0.22	-0.76	-0.74	-0.54	-0.52
1990-1999	-0.05	-0.06	-0.35	-0.45	-0.30	-0.39
2000-2019	0.22	0.22	0.83	0.91	0.61	0.69
2010-2019	0.42	0.45	1.51	1.68	1.09	1.23
2020-2024	0.69	0.78	2.08	2.42	1.39	1.64
Winter						
1980-1989	-0.10	-0.16	-0.47	-0.24	-0.37	-0.08
1990-1999	-0.02	-0.03	-0.56	-0.53	-0.54	-0.50
2000-2009	0.15	0.16	0.73	0.71	0.58	0.55
2010-2019	0.35	0.38	1.66	1.66	1.31	1.28
2020-2024	0.54	0.62	1.35	1.38	0.81	0.76
Spring						
1980-1989	-0.20	-0.14	-0.83	-0.68	-0.63	-0.54



1990-1999	-0.01	-0.04	0.23	0.13	0.24	0.17
2000-2009	0.16	0.14	0.36	0.36	0.20	0.22
2010-2019	0.40	0.40	1.40	1.37	1.00	0.97
2020-2024	0.58	0.60	1.37	1.16	0.79	0.56
Summer						
1980-1989	-0.18	-0.15	-0.34	-0.29	0.16	-0.14
1990-1999	-0.001	-0.01	-0.09	-0.09	0.091	-0.08
2000-2009	0.14	0.13	0.33	0.28	0.19	0.15
2010-2019	0.34	0.35	0.64	0.70	0.30	0.35
2020-2024	0.61	0.63	0.86	1.04	0.25	0.41

189 **Table 1: Average temperature anomalies (K; with respect to 1981-2010) for the Arctic (north of 60°N), the globe, and their difference**  
190 **for the BEST and ERA5 data.**

191 Results for autumn are examined first (Figure 3 (ERA5) and Supplemental Figure 3 (BEST data)). The description of the  
192 results apply to both datasets unless indicated otherwise. For the first two decades, 1980-1989 and 1990-1999, both the average  
193 global anomaly and the average Arctic anomaly are small and negative, with the Arctic anomalies actually more negative than  
194 the global value. Since 1980-1989 is (primarily) the first decade of the 1981-2010 baseline period, greater negative anomalies  
195 for the Arctic than the globe still indicate amplified warming in the Arctic. Likewise, as the middle of the baseline period,  
196 1990-1999 experiences the smallest anomalies. This pattern reverses starting in the 2000-2009 decade. What this is capturing  
197 is that early in the record, the poleward gradient in 2-meter temperatures was stronger than it is today; as AA evolves, the  
198 gradient obviously weakens.

199 For the first decade, 1980-1989, LAAs are generally small across the Arctic, with a mix of positive and negative values, but  
200 with the negative anomalies obviously dominating (not shown). The exception is in the Chukchi Sea, where strong negative  
201 LAA values of up to 3°C are found. Based on data from 1979-1996, Parkinson et al. (1999) showed downward trends in ice  
202 concentration in the Chukchi Sea of around 4% per decade. However, as the area had more sea ice in the 1980-1989 decade  
203 relative to the 1981-2010 climatology, it shows up as negative LAA values in Figure 3. As noted, in the 1990-1999 decade,  
204 both the Arctic average and the global average anomaly are at their minimum, since this decade is in the middle of the 1981-  
205 2010 baseline (Table 1). However, the difference between the 1990-1999 and the subsequent 2000-2009 decade is striking.  
206 Both the Arctic and global average anomalies are positive (Table 1, Figures 3 and S3). Positive LAA values encompass most  
207 of the Arctic. The largest positive LAA values lie in the Chukchi and East Siberian Seas, reflecting the continuing development  
208 through this decade of extensive open waters in September (Figures 3 and S3). Note that the first clear indication of the  
209 emergence of AA related to sea ice loss was based on data extending through the end of the 2000-2009 decade (Serreze et al.,  
210 2009; Screen et al., 2010a, b). Wang et al. (2017) similarly found the emergence of amplified temperature anomalies over the  
211 Arctic (60-90°N) compared to the northern mid-latitudes (30-60°N) in this decade. By the 2010-2019 decade, autumn LAA  
212 values of 3-5°C in the ERA5 data (2-4°C in the BEST data) are now prominent along the entire Eurasian coast and in the

213 Chukchi Sea; consistent with the continued increase in open water areas in September. Much smaller AA values encompass  
214 most of the rest of the Arctic.

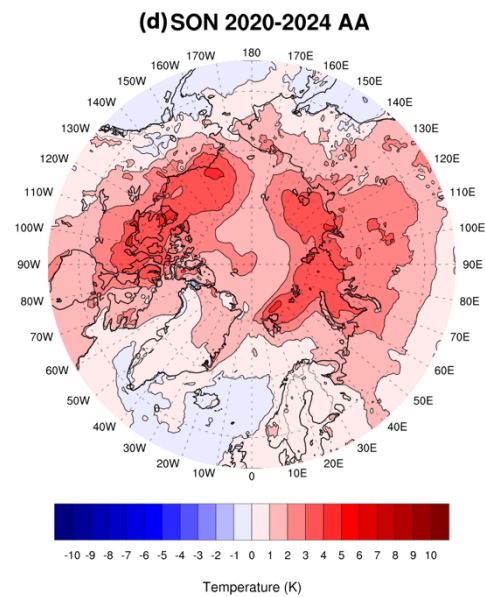
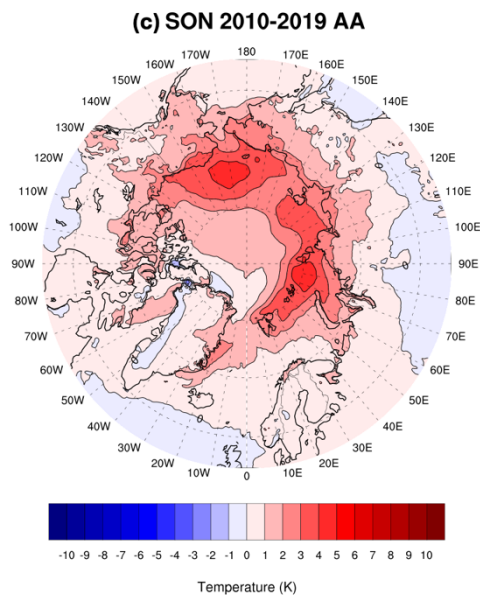
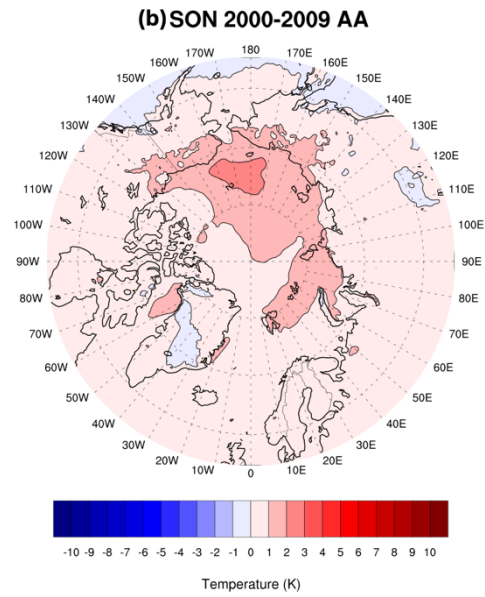
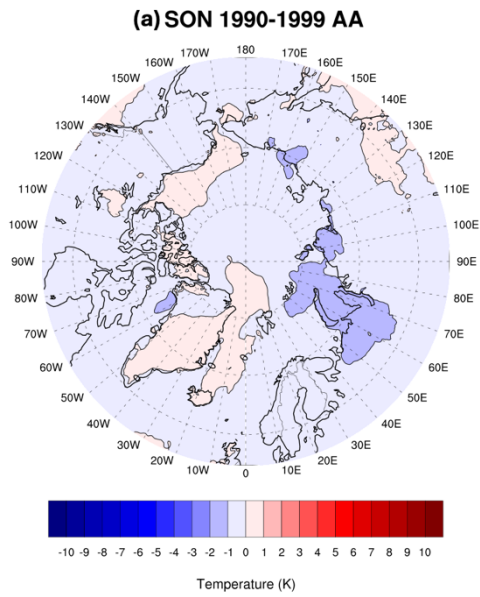
215 The most recent period, 2020-2024, sees a shift. While strongly positive anomalies relative to global average anomalies - that  
216 is, positive LAA values - remain over much of the Eurasian coastal sea, LAA anomalies over the Chukchi Sea are now smaller,  
217 and larger values have appeared in the Beaufort Sea and the Canadian Arctic Archipelago. In explanation, when Arctic sea ice  
218 extent began to decline, it was initially most prominent in the Chukchi Sea region, so LAA values there are especially large,  
219 as seen in the 2009-2009 and 2010-2019 plots. With the rise in the global temperature anomalies, these LAA values become  
220 more subdued.

221 The winter evolution is quite different. The Arctic-averaged anomaly and the global anomaly for the 1980-1989 are small and  
222 quite alike – AA had not yet emerged (Table 1). In terms of the LAA structure (not shown), positive values of typically 1-2°C  
223 over much of Eurasia, Alaska and Canada contrast with negative values of similar size elsewhere, the exception being negative  
224 values of 2-3°C in the Barents Sea sector. The story is similar for the 1990-1999 decade - AA had yet to clearly emerge (Table  
225 1), and, indeed, the Arctic average anomaly was about half a degree colder than the global average anomaly. The LAA structure  
226 leading to this interesting finding is characterized by partly offsetting positive and negative values (Figure 4 (ERA5) and  
227 Supplemental Figure 4 (BEST data)). As was the case for the discussion of the autumn AA, the description of the results  
228 applies to both datasets unless indicated otherwise. Of interest in this regard is that North Atlantic Oscillation (or Arctic  
229 Oscillation) shifted from a negative to a strongly positive index phase between the 1970s and late 1990s. Numerous studies  
230 examined the strong temperature trends associated with this shift, notably warming over northern Eurasia, with cooling over  
231 northeastern Canada and Greenland (e.g., Hurrell, 1995; 1996; Thompson and Wallace, 1998). There was vibrant debate over  
232 whether the shift might be in part a result of greenhouse gas forcing and an emerging signal of expected Arctic Amplification  
233 (see the review in Serreze et al., 2000).

234

235

236



237

238

239

240

**Figure 3. Autumn (September, October, November (SON)) ERA5 2-m temperature anomalies in °C relative to 1981-2010 for (a) 1990-1999, (b) 2000-2009, (c) 2010-2019 and (d) 2020-2024 minus the global average temperature anomaly for each period.**

241 While there is some indication of a structure in LAA values for the 1990-1999 decade reminiscent of the rising phase of the  
242 NAO over this time (note that the index value subsequently decreased), looking back to Table 1, the behavior of the NAO  
243 clearly did not “boost” any emerging AA signal.

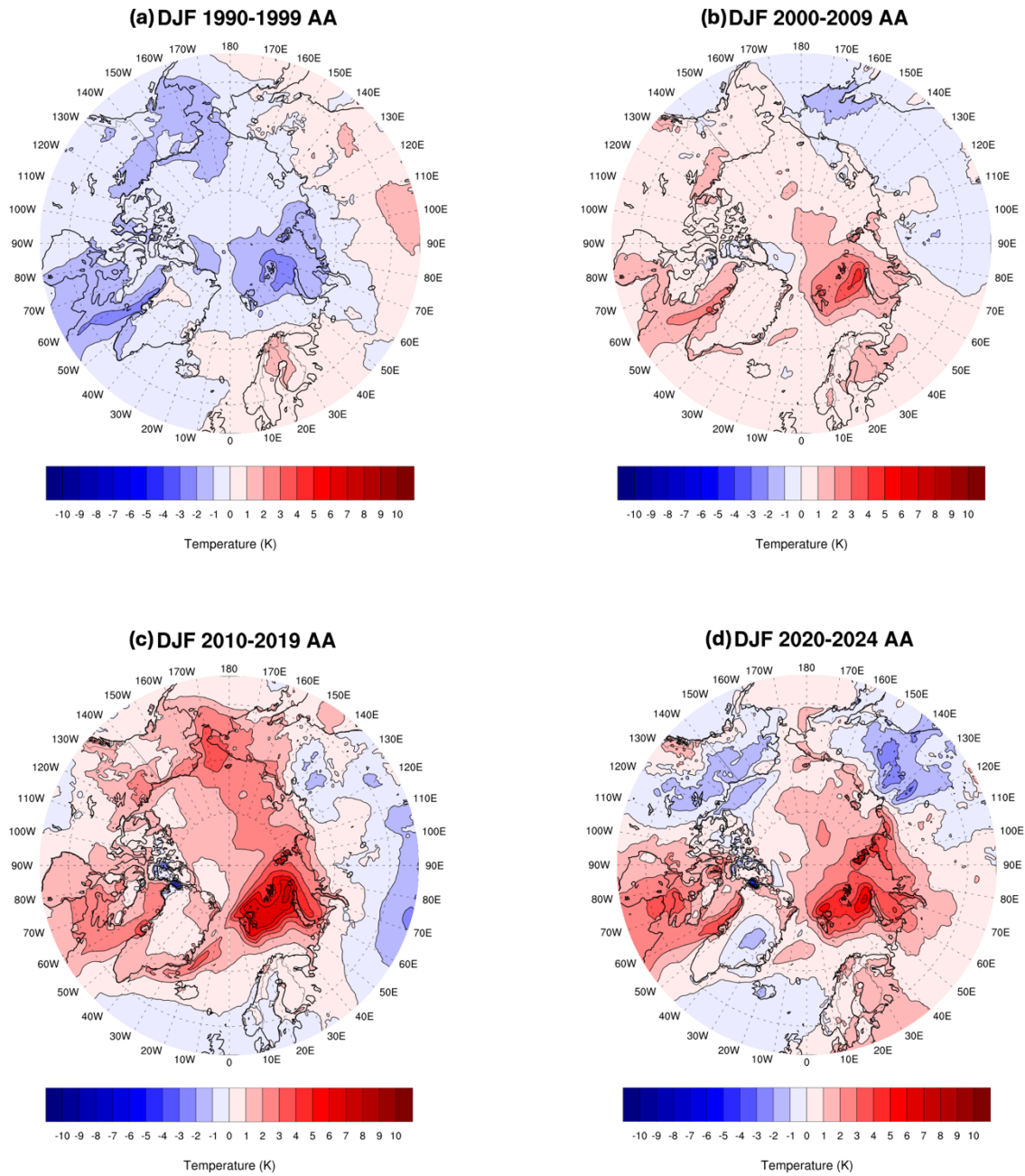
244 Turning to the decade 2000-2009, positive LAA values have become more dominant, and fairly large positive values have  
245 appeared over the Barents Sea sector, replacing the negative values of the previous decade. While by this decade, AA had  
246 clearly emerged (Table 1), note that the positive LAA values over northern Eurasia in 1990-1999 are replaced by negative  
247 values, indicative of a circulation shift, notably, regression of the NAO from its previous high index values.

248 The 2010-2019 period is characterized by the emergence of large positive LAA values over the Barents Sea sector which have  
249 intensified since the 2000-2009 decade, pointing to the effects of growing open water areas in this sector. Positive LAA values  
250 also cover almost all Arctic latitudes. The Barents Sea feature remains prominent in the past five years of the record (2020-  
251 2024). Note, however, the negative anomalies over Alaska and eastern Eurasia. As a result, the difference between the Arctic  
252 average temperature anomaly and the global average anomaly is actually smaller than in the 2010-2019 period, that is, pan-  
253 Arctic AA is somewhat smaller. Note also by comparison with the decade 2010-2019, LAA values along most of the Eurasia  
254 coast are less pronounced. This is understood in that, by December, all areas along the Eurasian coast and north of the Chukchi  
255 and East Siberian seas have refrozen.

256 The observation that the last three time periods have negative LAA values over Eurasia is of interest through its apparent link  
257 with Warm Arctic-Cold Eurasia (WACE) phenomenon -while AA has become increasingly prominent, this has been attended  
258 by recent surface cooling over Eurasia, most evident in winter with considerable decadal variability. (e.g., Gong et al., 2017;  
259 Li et al. 2021). The WACE phenomenon has garnered considerable attention over the past decades and a suite of driving  
260 factors have been offered. An Urals blocking pattern has been identified as playing a strong role, and recent work has shown  
261 that decadal variability in the WACE phenomenon is mediated by phases of the Pacific Oscillation and the Atlantic  
262 Multidecadal Oscillation (e.g., Luo et al., 2022).

263 Turning back to the Barents Sea sector, it is notable that this is one of the few areas of the Arctic (along with eastern Hudson  
264 Bay/Hudson Strait and Bering Strait, see Figure 2) with substantial downward trends in winter sea ice concentration. Various  
265 studies have attributed the loss of winter ice in the Barents Sea and associated temperature anomalies and trends to processes  
266 involving atmospheric circulation, facilitating intrusions of warm moist air into the region with wind patterns promoting  
267 stronger transport of warm Atlantic waters into the region (Woods and Caballero, 2016; Lien et al., 2017; Siew et al., 2024).  
268 Warm and moist air advection raises temperatures, inhibits autumn and winter sea ice growth (Woods and Caballero, 2016;  
269 Crawford et al., 2025; Lee et al., 2017), and enhances spring and summer ice melt (Kapsch et al., 2013; Park et al., 2015).  
270 Intrusions of Atlantic-derived waters, which appear to be in part wind driven, also discourage winter ice growth. Beer et al.

271 (2020) identified an oceanic mechanism that increases the vertical heat flux in the upper Arctic Ocean under global warming  
272 that causes increased ocean heat transport into the Arctic, which appears as a substantial contributor to Arctic Amplification.



273

274

275

276 **Figure 4: Winter (December, January, February, DJF) surface temperature anomalies in °C relative to 1981-2010 for (a) 1990-1999,**  
277 **(b) 2000-2009, (c) 2010-2019 and (d) 2020-2024 minus the global average temperature anomaly for each period.**

278 While our primary focus is on the evolution of AA and LAAs in autumn and winter, it is warranted to briefly discuss spring  
279 and summer (not shown). The spring pattern of LAAs for the 1980-1989 decade is characterized by small and mostly negative  
280 values across the Arctic, transitioning to a mix between small positive and negative values for the 1990-1999 decade, as well  
281 as for the 2000-2010 decade. The largest difference between the Arctic average and global average anomaly was for the 2010-  
282 2019 decade. This is consistent with the much smaller AA in this season compared to autumn and winter. Only for the last five  
283 years of the record, 2020-2024 do prominent positive LAA values of over 3°C appear over Eurasia, but these are partly  
284 balanced by negative LAAs elsewhere and may represent short-term internal variability. The key feature of summer is that  
285 while as the decades pass, modest positive values of LAA appear over land, values remain close to zero over the Arctic Ocean,  
286 reflecting the effects of the melting sea ice surface. The last five years also show positive LAA values of up to 3°C along the  
287 shores of Eurasia, likely due to the open coastal waters in these areas.

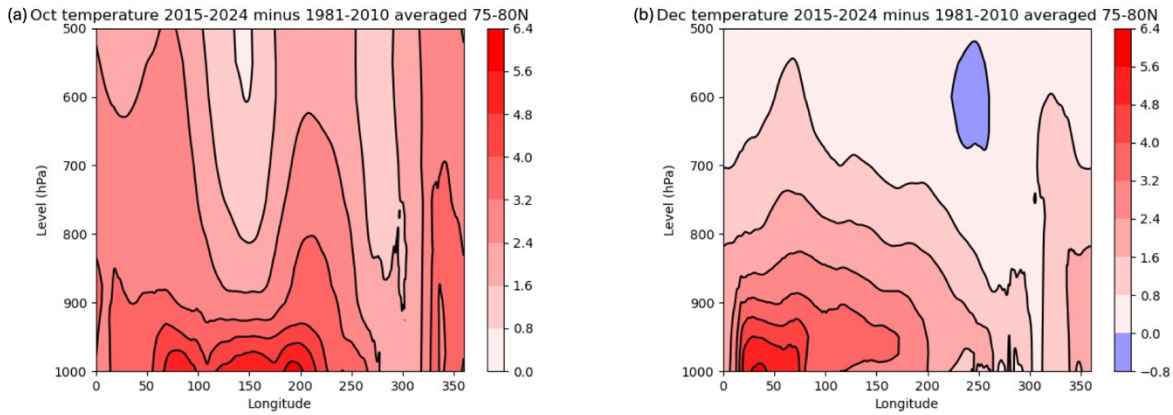
288 The results just discussed are with reference to 1981-2010 averages. Use of an earlier climatology (e.g., 1951-1980) naturally  
289 yields stronger positive anomalies and weaker negative LAA values in the later part of the temperature records, while a more  
290 recent climatology (e.g., 1991-2020, the current NOAA standard) has the opposite effect. The 1981-2010 reference applied  
291 in this paper is an appropriate middle ground, and is the reference period used for sea ice analyses by the National Snow and  
292 Ice Data Center (Scott, 2022).

### 293 **3.3 Vertical Structure**

294 An assessment of the vertical structure of warming helps to both highlight the effects of sea ice and shed light on other processes  
295 known to be involved in Arctic Amplification, notably, static stability. To this end, we look at longitudinal cross sections of  
296 temperature anomalies for the most recent 10 years of the record, averaged between the latitudes 75-80°N, which corresponds  
297 to the latitude band with pronounced anomalies in surface air temperature across both SON and DJF. We look first at October,  
298 then turn attention to December (Figure 5). October is when there will be particularly large heat fluxes from the ocean to  
299 atmosphere, while in December, most of these areas (apart from the Barents Sea) have re-frozen. This choice of months is  
300 intended to capture that contrast.

301 The strongly positive anomalies located from 60-120°E and between 180°E to 120°W (these being stronger) are clearly  
302 surface-based, which makes sense as they are due to strong upward surface heat fluxes. The more prominent feature between  
303 180°E and 120°W (centered along the East Siberian and Chukchi Seas) is notable in that anomalies of 3°C extend up to 700hPa.  
304 The December cross section shows maximum surface-based temperature anomalies focused between about 20-70°E (centered  
305 near the Barents Sea), but positive anomalies do not extend as far in the vertical compared to October. Although these

306 anomalies are less vertically extensive, the stronger near-surface temperature difference between the surface and the air above  
307 in December could potentially enhance surface fluxes.



308

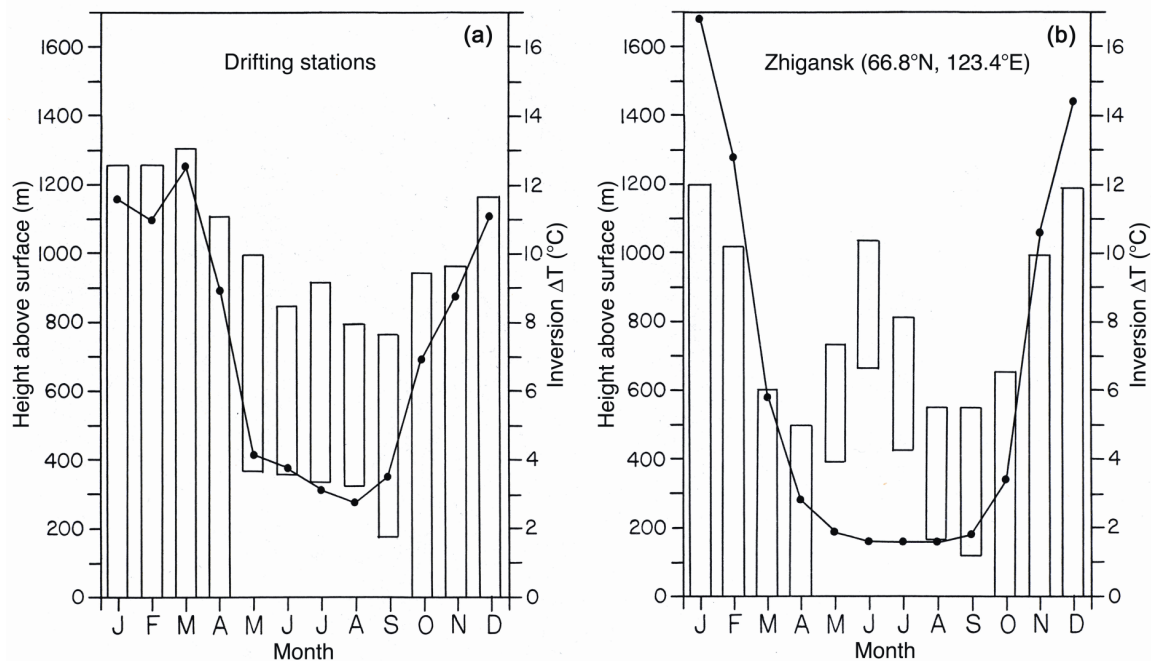
309 **Figure 5: Vertical cross sections by longitude across latitudes 75°N to 80°N for October (a) and December (b) of temperature**  
310 **anomalies for 2015-2024 minus 1981-2010.**

### 311 3.4 Static Stability

312 While the magnitude of the surface temperature anomaly will bear on how high in the vertical positive anomalies will persist,  
313 the vertical stability will play a role. The strong stability of the lower Arctic troposphere has long been recognized (Wexler,  
314 1936; Bradley et al., 1992; Kahl et al., 1992; Serreze et al., 1992) and is central to arguments that lapse rate feedback is a  
315 contributor to AA. Based on radiosonde observations, Serreze et al. (1992) reported that temperature inversions (extremely  
316 strong stability), nearly ubiquitous over the ice-covered Arctic Ocean, tend to be surface-based from October through April,  
317 increasing in strength from October through winter in both depth and in the temperature difference from inversion base to top.  
318 For example, in October the median inversion depth is about 900m and the temperature difference is about 9K, whereas  
319 corresponding values in March are 1200 m and 12K. In summer, inversions are shallower and often elevated, with a deep  
320 mixed layer below. (There are also commonly shallow melt-induced surface-based inversions.) The seasonal cycle over Arctic  
321 land areas is similar but with temperature differences across the inversion of 14-16K (Figure 6).

322 Figure 7 shows a vertical cross section of potential temperature from the equator to 90°N for October. Potential temperature  
323 increases with altitude more steeply in the Arctic than at other latitudes, illustrating its stronger static stability. In turn, a larger  
324 vertical extent of warming in October compared to December would be expected given that stability increases from autumn  
325 into winter. In terms of potential temperature, at 80°N (for example) the increase in potential temperature from the surface to  
326 850 hPa in October is 10K, versus 15K in December. From the surface to 700hPa, potential temperature increases by 20K in

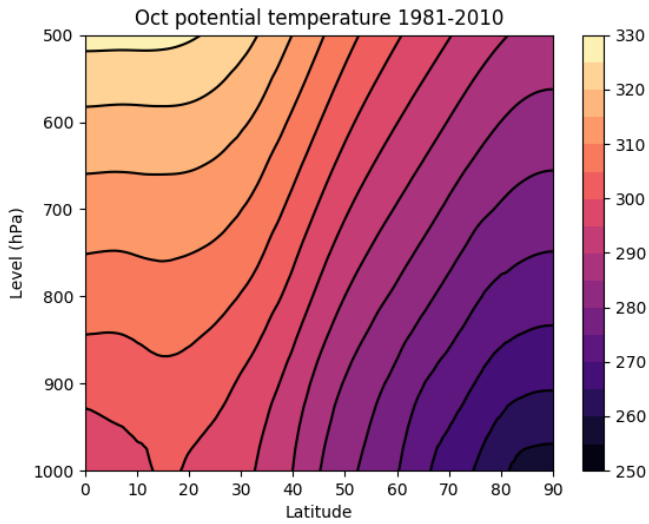
327 October versus 25K in December. The atmosphere starts to cool freely to space at around 5-6 km above the surface (roughly  
 328 the 500 hPa level). While pronounced autumn warming does not extend upwards that far (Figure 5), the results nevertheless  
 329 argue that as amplified warming progresses, cooling to space will become more efficient as a negative feedback on autumn  
 330 warming.



331

332 **Figure 6: Monthly median inversion top (top of bars), base (bottom of bars) and temperature difference (solid lines) from (a) drifting**  
 333 **station data from the central Arctic Ocean; (b) station Zhigansk over the Siberian tundra, taken as representative of the region**  
 334 **[from Serreze et al., 1992, by permission of AMS].**

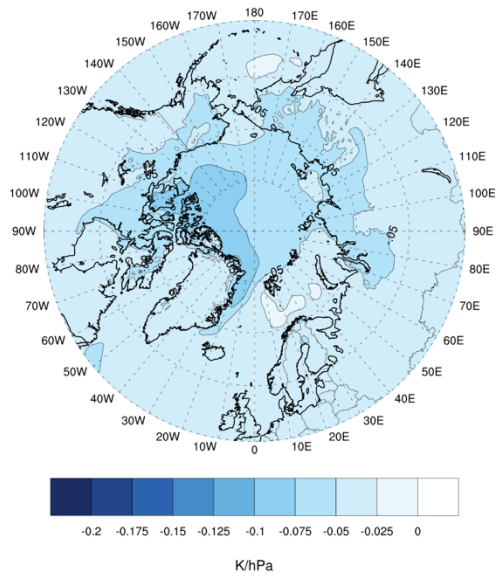




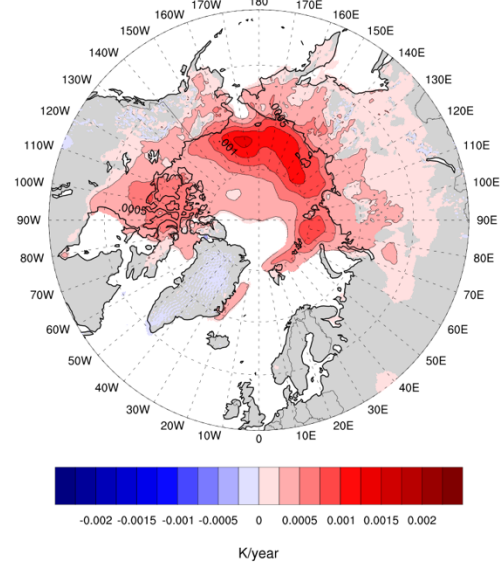
335

336 **Figure 7: Vertical cross section of zonally averaged potential temperature (K) from the equator to the pole for October, averaged**  
 337 **over the period 1981-2010.**

**(a) Oct Average  $d\theta/dp$  1000-850 hPa 1980-2024**



**(b) Oct trend in  $d\theta/dp$  /year 1000-850 hPa 1980-2024**



338

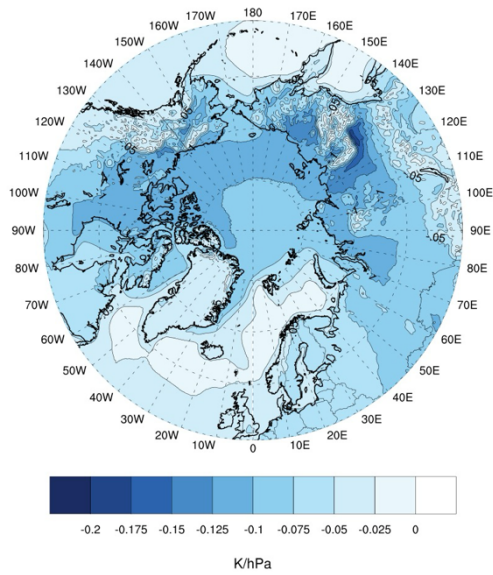
339 **Figure 8. Climatological averages (a, K/hPa) and linear trends (b, K/hPa per year) in low-level vertical stability (expressed as  $(\theta_{850}$**   
 340 **-  $\theta_{1000}) / (850 \text{ hPa} - 1000 \text{ hPa})$  for October. Positive numbers for the climatological averages mean weaker stability, positive values**  
 341 **for trends mean a decrease in stability with time. Only trends significant at  $p < 0.05$  are shaded based on an ordinary least squares**  
 342 **regression test.**

343 Figure 8 shows climatological averages of surface to 850 hPa static stability for October, along with linear trends. In a stable  
344 atmosphere,  $d\theta/dP$  is negative (potential temperature increases with height while pressure decreases), so more negative  
345 values mean stronger stability. Consistent with Figure 7, there is a general increase in average stability moving polewards.  
346 However, stability is strongest north of Greenland and the Canadian Arctic Archipelago. It is likely not a coincidence that  
347 these areas have the thickest sea ice in the Arctic, implying especially small heat fluxes through the ice. Not surprisingly, large  
348 trends toward weaker static stability (positive values) dominate all the areas along the Eurasian coast, corresponding to the  
349 largest declines in September ice concentration, as well as in the Barents Sea, which has seen declines in winter. Smaller trends  
350 towards weaker stability dominate most of the rest of the Arctic Ocean, likely driven by a thinning ice pack. While the average  
351 conductive heat flux through most of the ice cover in October is on the order of 5-10  $W m^{-2}$  (upward), Liu and Zhang (2025)  
352 found that the conductive heat flux has increased since 1979 due to thinning, which outcompetes the effect of positive trends  
353 in surface skin temperatures. Our analysis finds support in the study of Simmonds and Li (2021) who find strong decreases in  
354 the Brunt–Vaisalla frequency over the Arctic and its broader region. We note here that the B-V frequency contains a  $1/\theta$   
355 term which highlights the impact in the colder regions.

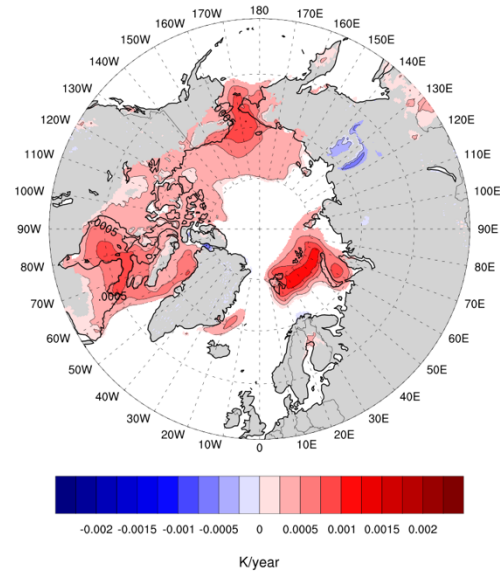
356 Corresponding results for December follow in Figure 9. Average stability is generally stronger than for October, with the clear  
357 exception of the Norwegian and Barents Seas and the extreme northern North Atlantic, where there is near neutral stability.  
358 The Norwegian and Barents Seas, in particular, have been recognized for unstable near-surface boundary layers in winter that  
359 develop during cold air outbreaks as Arctic air moves over open water surfaces, promoting strong surface heat fluxes and  
360 convective-type precipitation (Olafsson and Okland, 1994). Trends towards weaker stability are in turn prominent in the  
361 Barents Sea, the southern Chukchi Sea and Baffin and Hudson Bays, all areas where winter ice losses have been pronounced  
362 (especially the Barents Sea). Interesting in this regard is that weakening winter stratification may lead to intensification of near  
363 surface winds by increasing downward momentum transfer (Zapponini and Goessling, 2024), which will then foster stronger  
364 upward turbulent heat fluxes.

365 We stress that assessments of atmospheric stability and trends should be viewed with some caution. Based on comparisons  
366 with radiosonde profiles at coastal sites, Serreze et al. (2012) found that all three of the most modern reanalyses available at  
367 the time of that study (MERRA, NOAA CFSR, ERA-Interim) have positive cold-season temperature (and humidity) biases  
368 below the 850 hPa level and consequently did not capture observed low-level temperature and humidity and temperature  
369 inversions. MERRA had the smallest biases. Graham et al. (2019) similarly found a positive winter 2-m temperature bias in  
370 all six atmospheric reanalyses they compared to sea ice drifting stations – including ERA5. Additionally, Wang and Zhao  
371 (2024) found that the depiction of static stability over the Arctic in summer appears to be sensitive to the reanalysis product  
372 examined (ERA5, NCEP-R2 and JRA-55).

(a) Dec Average  $d\theta/dp$  1000-850 hPa 1980-2024



(b) Dec trend in  $d\theta/dp$  /year 1000-850 hPa 1980-2024



373

374 **Figure 9. Climatological averages (a, K/hPa) and linear trends (b, K/hPa per year) in low-level vertical stability (expressed as  $(\theta_{850} - \theta_{1000}) / (850 \text{ hPa} - 1000 \text{ hPa})$ ) for December. Positive numbers for the climatological averages mean weaker stability, positive values**  
375 **for trends mean a decrease in stability with time. Only trends significant at  $p < 0.05$  are shaded based on an ordinary least squares**  
376 **regression test.**  
377

#### 378 4 Discussion and Conclusions

379 The results presented here show a clear association between patterns of autumn and winter sea ice concentration trends and  
380 both the year-to-year evolution and seasonal expression of Arctic temperature anomalies. The link with sea ice loss can be  
381 viewed as an expression of seasonally delayed albedo feedback. We also see signals of variable atmospheric circulation in  
382 both temperature trends and the spatial structure of LAAs by decade. As discussed, a suite of other processes can also be linked  
383 to Arctic Amplification. Given that any process leading to warming will tend to enhance sea ice melt (spring and summer) or  
384 discourage its formation (autumn and winter), it can be viewed as serving to reinforce the key role of sea ice loss on observed  
385 AA.

386 Consider in this regard studies from coupled models showing that AA can arise without the albedo feedback through the lapse  
387 rate and Planck feedbacks (e.g., Caballero and Langen, 2005; Pithan and Mauritsen, 2014; Previdi et al., 2021). Lapse rate  
388 feedback relates to the stronger stability of the Arctic atmosphere compared to low latitudes, focusing the temperature rise  
389 closer to the surface and reducing longwave radiative cooling to space. From coupled simulations, Previdi et al. (2021) find  
390 that through positive lapse rate feedback, AA develops in only a few months following an instantaneous quadrupling of

391 atmospheric CO<sub>2</sub>, well before any significant sea ice loss, although ice loss contributes significantly to warming after the first  
392 few months. While one can question what an instantaneous quadrupling of CO<sub>2</sub> teaches us about the real world, a key point is  
393 once sea ice begins to decline, the positive lapse rate feedback, keeping the heating near the surface, will contribute to spring  
394 and summer ice melt and delay seasonal ice growth. That static stability becomes stronger from autumn into winter indicates  
395 that focusing the heating near the surface will also be more effective in winter. Conversely, ice loss, and likely also heat fluxes,  
396 are changing the larger environment towards reduced stability at low levels.

397 Turning to the Planck feedback, the larger increase in Arctic temperatures required to bring the system back to radiative  
398 equilibrium in response to a forcing can also be seen as a process augmenting summer sea ice loss and delaying autumn and  
399 winter ice growth. Increased autumn cloud cover as a contributor to AA is closely tied to sea ice loss through reducing stability  
400 in the boundary layer, promoting large upward surface heat fluxes (e.g., Kay and Gettleman, 2012).

401 In parting, a key message stemming from the present study is that the process of AA must consider both its strong seasonality  
402 and that AA, which is generally assessed by comparing Arctic regional temperature trends against trends for the globe as a  
403 whole, comes about by the integration across the Arctic of large spatial heterogeneity of temperature changes, seen both in the  
404 spatial pattern of Arctic trends but especially when we look at the problem through local amplification anomalies – LAAs.  
405 While AA is small in summer, summer processes, namely the reduction of sea ice concentration and enhanced energy gain in  
406 the mixed layer, set the stage for the strong regional expressions of AA in autumn. These changes in spatial patterns of  
407 temperature anomalies extend into winter as areas of open water freeze over. In all seasons, variable atmospheric circulations  
408 appear to be important. Anomalous summer circulation can affect spatial patterns of September ice extent. In autumn and  
409 winter, these anomalous circulation patterns can affect temperature through advection as well as by their influence on sea ice  
410 concentration, such as in the Barents Sea. Static stability also changes seasonally, which will influence the vertical expression  
411 of temperature anomalies.

412 In short, the more we look at AA, the more we discover that it is a very complex beast. These complexities bear not only on  
413 the future evolution of AA and related impacts on permafrost warming and changes in the frequency of rain on snow events  
414 (Serreze et al., 2021), but on key issues such as potential impacts of Arctic warming on middle latitude weather patterns (Ding  
415 et al., 2024).

416 *Code and data availability:* The ERA5 data were obtained from the Research Data Archive at the National Center for  
417 Atmospheric Research: DOI: 10.5065/BH6N-5N20. Sea ice data was obtained from the National Snow and Ice Data Center  
418 <https://nsidc.org/data/nsidc-0051/versions/2>. For processing code contact Elizabeth Cassano  
419 (Elizabeth.Cassano@colorado.edu)

420 *Author contributions:* Mark Serreze wrote the first draft of the paper. Elizabeth Cassano performed the bulk of the data analysis  
421 and creation of figures and assisted in writing. Alex Crawford, John Cassano and Chen Zhang provided intellectual input to  
422 the paper and contributed to the writing.

423 *Competing interests.* The contact author has declared that none of the authors has any competing interests.

424 *Acknowledgement:* This study was supported by NSF Navigating the New Arctic Grant 1928230 and the Canada-150 Chair  
425 Program.

426

## 427 **References**

428 AMAP, Arctic Climate Change Update 2021: Key trends and impacts. Summary for policy-makers, Arctic Monitoring and  
429 Assessment Programme (AMAP), Oslo, Norway, 2021.

430 Arrhenius, 1896: On the influence of carbonic acid in the air upon the temperature of the ground. *Philos. Mag. J. Sci.*, 5, 237-  
431 276.

432 Barrett, A.P., Stroeve, J.C., and Serreze, M.C.: Arctic Ocean Precipitation from atmospheric reanalyses and comparisons with  
433 North Pole drifting station records, *Journal of Geophysical Research: Oceans*, 125(1). <https://doi.org/10.1029/2019jc015415>,  
434 2020.

435 Beer, E., Eisenman, I., and Wagner, T. J.: Polar amplification due to enhanced heat flux across the halocline, *Geophys. Res.*  
436 *Let.*, 47, <https://doi.org/10.1029/2019GL086706>, 2020.

437 Bianco, E., Lovino, D., Masina, S., Materia, S., and Ruggieri, P.: The role of upper-ocean heat content in the regional variability  
438 of Arctic sea ice at sub-seasonal timescales, *The Cryosphere*, 18, 2357–2379, <https://doi.org/10.5194/tc-18-2357-2024>, 2024.

439 Bradley, R.S, Kemig, F.T. and Diaz, H.F.: Climatology of surface-based inversions in the North American Arctic, *J. Geophys.*  
440 *Res. Atmospheres*, 97(D14), 15699- 15712, <https://doi.org/10.1029/92JD01451>, 1992.

441 Caballero, R., and Langen, P.: The dynamic range of poleward energy transport in an atmospheric general circulation model,  
442 *Geophys. Res. Lett.*, 32, L02705, [doi:10.1029/2004GL021581](https://doi.org/10.1029/2004GL021581), 2025.

443 Crawford, A. D., Lukovich, J. V., McCrystall, M. R., Stroeve, J. C., and Barber, D. G.: Reduced sea ice enhances intensification  
444 of winter storms over the Arctic Ocean, *J. Climate*, 35(11), 3353–3370. <https://doi.org/10.1175/jcli-d-21-0747.1>, 2022.

445 Crawford, A., Soriot, C., and Stroeve, J.: Autumn pauses in Arctic-wide sea-ice expansion, *J. Glaciol.*, 71, e21,  
446 <https://doi.org/10.1017/jog.2024.106>, 2025.

447 Dai, A., Luo, D., Song, M., and Liu, J.: Arctic amplification is caused by sea-ice loss under increasing CO<sub>2</sub>, *Nat. Comm.*, 10,  
448 121, <https://doi.org/10.1038/s41467-018-07954-9>, 2019.

449 Ding, S.S., Chen, X., Zhang, X., Zhang, X., and Xu, P.: A review on the Arctic-midlatitudes connection: Interactive impacts,  
450 physical mechanisms and nonstationary, *Atmosphere*, 15, 20.33980/atmosph15091115, 2024.

451 Esau, I., Pettersson, L. H., Cancet, M., Chapron, B., Chernokulsky, A., Donlon, C., Johannesen, J. A.: The arctic  
452 amplification and its impact: A synthesis through satellite observations. *Remote Sensing*, 15(5), 1354, 2023..

453 Fetterer, F., Knowles, K., Meier, W., and Savoie, M.: Sea Ice Index, digital media, National Snow and Ice Data Center,  
454 Boulder, Colorado, 2002.

- 455 Gong, T., Feldstein, S., and Lee, S.: The role of downward infrared radiation in the recent Arctic winter warming trend. *J.*  
456 *Climate*, **30**, 4937–4949, <https://doi.org/10.1175/JCLI-D-16-0180.1>, 2017.
- 457 Graham, R. M., Cohen, L., Ritzhaupt, N., Segger, B., Graversen, R. G., Rinke, A., et al.: Evaluation of six atmospheric  
458 reanalyses over Arctic sea ice from winter to early summer, *J. Climate*, **32**(14), 4121–4143, <https://doi.org/10.1175/jcli-d-18->  
459 0643.1, 2019.
- 460 Graversen, R. G., and Burtu, M. Arctic amplification enhanced by latent energy transport of atmospheric planetary waves,  
461 *Quart. J. Roy. Meteor. Soc.*, **142**, 2046–2054, 2016.
- 462 Henderson, G. R., Barrett, B. S., Wachowicz, L. J., Mattingly, K. S., Preece, J. R., and Mote, T. L.: Local and remote  
463 atmospheric circulation drivers of Arctic change: A review. *Frontiers in Earth Science*, **9**, 709896, 2021.
- 464 Hersbach and Coauthors: The ERA5 global reanalysis, *Quart. J. Roy. Meteor. Soc.*, **146**, 1999–2049,  
465 <https://doi.org/10.1002/qj.3803>, 2020.
- 466 Hurrell, J.W.: Decadal trends in the North Atlantic Oscillation: Regional temperatures and precipitation, *Science* , **269**,  
467 676-679, 1995.
- 468 Hurrell, J.W.: Influence of variations in extratropical wintertime teleconnections on Northern Hemisphere temperature,  
469 *Geophys. Res. Lett.*, **23**, 665-668, 1996.
- 470 Jansen, E., Christensen, J.H., Dokken, T., Nisancioglu, K.H., Vintgher, B.M., Capron, E., Guo, C., Jensen, M.F., Langen,  
471 P.L., Pedersen, R.A., Yang, S., Bentsen, M., Kjaer, H.A., Sadatzki, H., Sessford, E., and Stendel, M.: Past perspectives on the  
472 present era of abrupt Arctic climate change, *Nat. Clim. Change*, **10**, 714–721, 2020.
- 473 Kahl, J.D., Serreze, M.C., and Schnell, R.C.: Tropospheric low-level temperature inversions in the Canadian Arctic,  
474 *Atmosphere-Ocean*, **30**, 522-529, <https://www.tandfonline.com/doi/abs/10.1080/07055900.1992.9649453>, 1992
- 475 Kapsch, M.-L., Graversen, R.G., and Tjernström, M.: Springtime atmospheric energy transport and the control of Arctic  
476 summer sea-ice extent, *Nat. Climate Change*, **3**, 744–748, doi:10.1038/nclimate1884, 2013.
- 477 Kay, J. E., and Gettelman, A.: Cloud influence on and response to seasonal Arctic sea ice loss, *J. Geophys. Res.*, **114**, D18204,  
478 doi:10.1029/2009JD011773, 2009
- 479 Krishnan, S. et al.: The roles of the atmosphere and ocean in driving Arctic warming due to European aerosol reductions,  
480 *Geophys. Res. Lett.*, **47**, e2019GL086681, 2020.
- 481 Landy, J. C., Dawson, G. J., Tsamados, M., Bushuk, M., Stroeve, J. C., Howell, S. E. L., Krumpen, T., Babb, D. G., Komarov,  
482 A. S., Heorton, H. D. B. S., Belter, H. J., and Aksenov, Y.: A year-round satellite sea-ice thickness record from CryoSat-2,  
483 *Nature*, **609**, 517–522, <https://doi.org/10.1038/s41586-022-05058-5>, 2022.
- 484 Lebrun, M., M. Vancoppenolle, Madec, G., and Massonnet, F.: Arctic sea-ice-free season projected to extend into autumn.  
485 *The Cryosphere*, **13**, 79–96, <https://doi.org/10.5194/tc-13-79-2019>, 2019.
- 486
- 487 Lee, S., Gong, T., Feldstein, S. B., Screen, J. A., and Simmonds, I. Revisiting the cause of the 1989–2009 Arctic surface  
488 warming using the surface energy budget: Downward infrared radiation dominates the surface fluxes. *Geophysical Research*  
489 *Letters*, **44**(20), 10-654, 2017
- 490
- 491 Li, M., Lui, D., Simmonds, A., Dai A., Zhong, L. and Yao, Y., 2021: Anchoring of atmospheric teleconnection patterns by  
492 Arctic Sea ice loss and its link to winter cold anomalies in East Asia, *Int. J. Climatol.*, **41**, 547–558, 2021.
- 493 Li, Z., Ding, Q., Steele, M., and Schweiger, A.: Recent upper Arctic Ocean warming expedited by summertime atmospheric  
494 processes, *Nat. Commun.*, **13**, 362, <https://doi.org/10.1038/s41467-022-28047-8>, 2022.

- 495 Lien, V. S., Schlichtholz, P., Skagseth, Ø., and Vikebø, F. B.: Wind-driven Atlantic water flow as a direct mode for reduced  
496 Barents Sea ice cover, *Journal of Climate*, 30, 803–812, <https://doi.org/10.1175/jcli-d-16-0025.1>, 2017.
- 497 Liu, Y., and Zhang, J.: Conductive heat flux over Arctic sea ice from 1979 to 2022. *J. Geophys. Res.* 130: e2024JC022062  
498 doi: 10.1029/2024JC022062, 2025.
- 499 Luo, B., Luo, D., Dai, A., Simmonds, I., and Wu., L.: Decadal variability of winter warm Arctic-cold Eurasia dipole patterns  
500 modulated by Pacific Decadal Oscillation and Atlantic Multidecadal Oscillation. *Earth's Future*, 10, e2021EF002351, doi:  
501 10.1029/2021EF002351, 2022.
- 502 Markus, T., J. C. Stroeve, J.C., and Miller, J.: Recent changes in Arctic sea ice melt onset, freezeup, and melt season length.  
503 *Journal of Geophysical Research*, 114, C12024, <https://doi.org/10.1029/2009jc005436>, 2009.
- 504 Mudryk, L.R., Chereque, A.E., Derksen, C., Loujus K. and Decharme, B.: Terrestrial Snow Cover, NOAA Arctic Report Card  
505 2023, doi: 10.25923/xqwa-h543, 2023.
- 506 Navarro, J.A., Varma, V., Riipinen, I., Seland, O., Kirkevåg, A., Struthers, H., Iversen, T., Hansson, H.-C., and Ekman,  
507 A.M.L.: Amplification of Arctic warming by past air pollution reductions in Europe, *Nature Geosci.*, 9, 277–281,  
508 <https://doi.org/10.1038/ngeo2673>, 2016.
- 509 Olafsson, H., and Okland, E.: Precipitation from convective boundary layers in Arctic air masses, *Tellus A*, 46, 4–13,  
510 <https://doi.org/10.3402/tellusa.v46i1.15422>, 1994.
- 511 Park, H.-S., Lee, S., Kosaka, Y., Son, S.-W., and Kim, S.-W.: The impact of Arctic winter infrared radiation on early summer  
512 sea ice, *J. Climate*, 28, 6281–6296, doi:10.1175/JCLI-D-14-00773.1, 2015.
- 513 Parkinson, C.L., Cavalieri, D.J., Gloersen, P., Zwally, H.J., and Comison, J.C.C., Arctic sea ice extent, areas and trends, 1989-  
514 1996, *J. Geophys. Res.*, 104, 20,837-20, 856, 1999.
- 515 Perovich, D. K. and Polashenski, C.: Albedo evolution of seasonal Arctic sea ice, *Geophys. Res. Lett.*, 39, 8,  
516 <https://doi.org/10.1029/2012GL051432>, 2012.
- 517 Perovich, D.K., Light, B., Eicken, H., Jones, K.F. Runcimen, K. and Nghiem, S.V.: Increasing solar heating of the Arctic Ocean  
518 and adjacent seas, 1979–2005: Attribution and the role of ice-albedo feedback, *Geophys. Res. Lett.*, 34, L19505, doi:  
519 10.1029/2007GL031480, 2007.
- 520 Pithan, F., and Mauritsen, T.: Arctic amplification dominated by temperature feedbacks in contemporary climate models,  
521 *Nature Geosci.*, 7, 181–184, <https://doi.org/10.1038/ngeo2071>, 2014.
- 522 Previdi, M., Smith, K.L., and Polvani, L.M.: Arctic amplification of climate change: a review of underlying mechanisms.  
523 *Env. Res. Lett.*, 16, 093003, doi:10.1088/1748-9326/ac1c29, 2021.
- 524 Rantanen M., Karpechko A.Y., Lipponen, A., Nordling, K., Hyvärinen, O., Ruosteenoja, K., Vihma T., and Laaksonen, A.:  
525 The Arctic has warmed nearly four times faster than the globe since 1979, *Nature Communications Earth and Environment*, 3,  
526 168, <https://doi.org/10.1038/s43247-022-00498-3>, 2022.
- 527 Renfrew, I. A., Barrell, C., Elvidge, A. D., Brooke, J. K., Duschka, C., King, J. C., et al.: An evaluation of surface meteorology  
528 and fluxes over the Iceland and Greenland Seas in ERA5 reanalysis: The impact of sea ice distribution, *Quart. J. Roy. Meteor.*  
529 *Soc.*, 147(734), 691–712, <https://doi.org/10.1002/qj.3941>, 2021.
- 530 Richter-Menge, J., and Druckenmiller, M. L. (eds.) The Arctic [In “State of the Climate in 2019“], *Bull. Am. Meteor. Soc.*,  
531 101, S239–S285, 2020.
- 532 Rohde, R.A., and Hausfather, Z.: The Berkeley Earth Land/Ocean Temperature Record. *Earth Sys. Sci. Data.*, 12, 3469-3479,  
533 <https://doi.org/10.5194/essd-12-3469-2020>, 2020.
- 534 Scott, M. “Why use the 1981 to 2010 average for sea ice?” National Snow and Ice Data Center. Accessed 11 Sep  
535 2025. <https://nsidc.org/learn/ask-scientist/why-use-1981-2010-average-sea-ice>, 2022.

536 Screen, J.A., and Simmonds, I.: The central role of diminishing sea ice in recent Arctic temperature amplification, *Nature*, 464,  
537 1334–1337, doi:10.1038/nature09051, 2010a.

538 Screen, J., and I. Simmonds: Increasing fall–winter energy loss from the Arctic Ocean and its role in Arctic temperature  
539 amplification. *Geophys. Res. Lett.*, 37, L16707, doi:10.1029/2010GL044136, 2010b.

540 Serreze, M.C., Kahl, J.D. and Schnell, R.C.: Low level temperature inversions of the Eurasian Arctic and comparisons with  
541 Soviet drifting station data, *J. Climate*, 5, 615–629, [https://doi.org/10.1175/1520-0442\(1992\)005<0615:LLTIOT>2.0.CO;2](https://doi.org/10.1175/1520-0442(1992)005<0615:LLTIOT>2.0.CO;2),  
542 1992. [https://journals.ametsoc.org/view/journals/clim/5/6/1520-0442\\_1992\\_005\\_0615\\_lltlot\\_2\\_0\\_co\\_2.pdf](https://journals.ametsoc.org/view/journals/clim/5/6/1520-0442_1992_005_0615_lltlot_2_0_co_2.pdf), 1992.

543 Serreze, M.C., Walsh, J.E., Chapin, F.S., III, Osterkamp, T., Dyurgerov, M., Romonovsky, V., Oechel, W.C., Morison, J.,  
544 Zhang, T., and Barry, R.G.: Observational evidence of recent change in the northern high latitude environment, *Climatic*  
545 *Change*, 46, 159–207, 2000.

546 Serreze, M., Barrett, A., Stroeve, J., Kindig, D., and Holland, M.: The emergence of surface-based Arctic amplification,  
547 *Cryosphere*, 3, <https://doi.org/10.5194/tc-3-11-2009>, 2009.

548 Serreze, M.C., Barrett, A.P., and Stroeve, J.: Recent changes in tropospheric water vapor over the Arctic as assessed from  
549 radiosondes and atmospheric reanalyses. *Journal of Geophysical Research*, 117, D10104, doi: 10.1029/2011JD017421, 2012.

550 Serreze, M.C., Gustavson, J., Barrett, A.P., Druckenmiller, M.L., Fox, S., Voveris, J., Stroeve, J., Sheffield, B., Forbes, B.C.,  
551 Rasmus, S., Laptander, R., Brook, M., Brubaker, M., Temte, J., McCrystal, M., and Bartsch, A.: Arctic rain on snow events:  
552 bridging observations to understand environmental and livelihood impacts. *Environmental Research Letters*, 16,  
553 <https://doi.org/10.1088/1748-9326/ac269b>, 2021

554 Siew, P.Y.F., Wu, Y., Ting, M., Zheng, C., Ding, O. and Seager, R.: Significant contribution of internal variability to recent  
555 Barents–Kara sea ice loss in winter, *Comm. Earth Environ.*, 5, 411, <https://doi.org/10.1038/s43247-024-01582-6>, 2024.

556 Simmonds, I. And Li, M.: Trends and variability in polar sea ice, global atmospheric circulations, and baroclinicity *Ann. NY*  
557 *Acad. Sci.* **1504** 167–86, 2021.

558 Smith, D.M., J.A. Screen, C. Deser, J. Cohen, J.C. Fyfe, J. García-Serrano, T. Jung, V. Kattsov, D. Matei, R. Msadek, Y.  
559 Peings, M. Signmond, J. Ukita, J.-H. Yoon, and X. Zhan: The Polar Amplification Model Intercomparison Project (PAMIP)  
560 contribution to CMIP6: investigating the causes and consequences of polar amplification, *Geosci. Model Dev.*, 12, 1139–1164,  
561 <https://doi.org/10.5194/gmd-12-1139-2019>, 2019.

562 Stammerjohn, S., Massom, R. Rind, D., and Martinson, D.: Regions of rapid sea ice change: An inter-hemispheric seasonal  
563 comparison, *Geophys. Res. Lett.*, 39, L06501, doi: 10.1029/2012GL080874, 2012.

564 Steele, M., Ermold, W., and Zhang, J.: Arctic Ocean surface warming trends over the past 100 years, *Geophys. Res. Lett.*, 35,  
565 L02614, doi:10.1029/2007GL031651, 2008.

566 Stroeve, J. and Notz, D.: Changing state of Arctic sea ice across all seasons, *Env. Res. Lett.*, 13, 10300,  
567 <https://doi.org/10.1088/1748-9326/aade56>, 2018.

568 Stroeve, J.C., Markus, T., Boisvert, L., Miller, J., and Barrett, A.: Changes in Arctic melt season and implications for sea ice  
569 loss, *Geophys. Res. Lett.*, 41, 1216–1225, doi:10.1002/2013GL058951, 2014.

570 Stroeve, J. C., A. D. Crawford, and S. Stammerjohn: Using timing of ice retreat to predict timing of fall freeze-up in the Arctic.  
571 *Geophysical Research Letters*, 43, 6332–6340, <https://doi.org/10.1002/2016gl069314>, 2016.

572 Stuecker, M. F., Bitz, C.M., Armour, K.C., Proistosescu, Kang, S.M., Shang-Ping, Xie, Doyeon, K., McGregor, S., Zhang, W.,  
573 Zhao, S., Cai, W., Dong, Y. and Jin, F-F.: Polar amplification dominated by local forcing and feedbacks, *Nat. Clim. Change*,  
574 8, 1076–1081, 2018.

575 Sumata, H., Steur, L. de, Divine, D. V., Granskog, M. A., and Gerland, S.: Regime shift in Arctic Ocean sea ice thickness,  
576 *Nature*, 615, 443–449, <https://doi.org/10.1038/s41586-022-05686-x>, 2023.



577 Taylor, P. C., Boeke, R. C., Boisvert, L. N., Feldl, N., Henry, M., Huang, Y., and Tan, I.: Process drivers, inter-model spread,  
578 and the path forward: A review of amplified Arctic warming. *Frontiers in Earth Science*, 9, 758361, 2022. Thompson, D.W.J.,  
579 and Wallace, J.M.: The Arctic Oscillation signature in the wintertime geopotential height and temperature fields, *Geophys.*  
580 *Res. Lett.* 25, 1297-1300, 1998.

581 Tian, T., Yang, S., Høyer, J. L., Nielsen-Englyst, P., and Singha, S.: Cooler Arctic surface temperatures simulated by  
582 climate models are closer to satellite-based data than the ERA5 reanalysis. *Communications Earth & Environment*, 5(1),  
583 111, 2024.

584 Timmermans, M.-L., Toole, J., and Krishfield, R.: Warming of the interior Arctic Ocean linked to sea ice losses at the basin  
585 margins, *Sci. Adv.*, 4, eaat6773, <https://doi.org/10.1126/sciadv.aat6773>, 2018.

586 Walsh, J. E.: Intensified warming of the Arctic: Causes and impacts on middle latitudes, *Glob. Planet. Change* 117, 52–63,  
587 2014.

588 Wang, X. and Zhao, J.: Trends and oscillations in arctic mediterranean atmospheric static stability during recent Arctic  
589 warming. *Climate and Atmospheric Science*, <https://www.nature.com/articles/s41612-024-00576-7>, 2024.

590 Wang, Y., F. Huang, and T. F.: Spatio-temporal variations of Arctic amplification and their linkage with the Arctic oscillation.  
591 *Acta Oceanol. Sin.*, 36, 42–51, <https://doi.org/10.1007/s13131-017-1025-z>, 2017.

592 Wang, C., Graham, R. M., Wang, K., Gerland, S., and Granskog, M. A.: Comparison of ERA5 and ERA-Interim near-  
593 surface air temperature, snowfall and precipitation over Arctic sea ice: effects on sea ice thermodynamics and evolution. *The*  
594 *Cryosphere*, 13(6), 1661-1679, 2019

595 Wexler, H.: Cooling in the lower atmospheric and the structure of polar continental air, *Mon. Wea. Rev.*, 64, 122-136, 1936.

596 Woods, C. and Caballero, R.: The role of moist intrusions in winter Arctic warming and sea ice decline, *J. Clim.*, 29, 4473–  
597 4485, <https://doi.org/10.1175/JCLI-D-15-0773.1>, 2016.

598 Wu, D.L., and Lee, J.N.: Arctic low cloud changes as observed by MISR and CALIOP: Implication for the enhanced autumnal  
599 warming and sea ice loss, *J. Geophys. Res.*, 117, D07107, doi: 10.2029/2011JD017040, 2012.

600 Yu, L., Zhong, S., Vihma, T., and Sun, B.: Attribution of late summer early autumn Arctic sea ice decline in recent decades,  
601 *npj Clim. Atmos. Sci.* 4, 3, 2021a.

602 Yu, Y., Xiao, W., Zhang, Z., Cheng, X., Hui, F., and Zhao, J.: Evaluation of 2-m air temperature and surface temperature  
603 from ERA5 and ERA-I using buoy observations in the Arctic during 2010–2020. *Remote Sensing*, 13(14), 2813, 2021b.

604 Zapponini, M., and Goessling, H.F.: Atmospheric destabilization leads to Arctic Ocean winter surface wind intensification,  
605 *Nature Communications Earth and Environment*, <https://doi.org/10.1038/s43247-024-01428-1>, 2024.

606 Zhang, C., Cassano, J. J., Seefeldt, M. W., Wang, H., Ma, W., and Tung, W.: Quantifying the impacts of atmospheric rivers  
607 on the surface energy budget of the Arctic based on reanalysis, *The Cryosphere*, 19, 4671–4699, [https://doi.org/10.5194/tc-](https://doi.org/10.5194/tc-19-4671-2025)  
608 19-4671-2025, 2025.

609 Zhou, W., Yao, Y., Luo, D., Simmonds, I., and Huang, F.: The key atmospheric drivers linking regional Arctic amplification  
610 with East Asian cold extremes. *Atmos. Res*, 283, 106557, doi: 10.1016/j.atmosres.2022.106557, 2023

611 Zhou, W., Leung, L. R., and Lu, J.: Steady threefold Arctic amplification of externally forced warming masked by natural  
612 variability. *Nat. Geosci.*, 17, 508–515, <https://doi.org/10.1038/s41561-024-01441-1>, 2024.